Journal of the Brazilian Society of Mechanical Sciences and Engineering (2023) 45:50
https://doi.org/10.1007/s40430-022-03978-x

TECHNICAL PAPER

A modified coupling Independent Component Analysis algorithm applied to a semi-active suspension system

Dorra Ben Hassen[1] · Maroua Haddar[1] · Anoire Ben Jdidia[1] · Mohamed Slim Abbes[1] · Mohamed Haddar[1]

Received: 7 April 2022 / Accepted: 19 December 2022 / Published online: 31 December 2022

Abstract

In this paper, the Independent Component Analysis (ICA) was proposed to be integrated with a semi-active control in order to improve the vehicle performance in real time. In fact the ICA was used to estimate the road profile variability. Taking into account the estimated road information, a skyhook controller was allowed to switch its control gain. It acts accurately in real time to eliminate the vibrations and ensure passengers comfort. This control was used due to its simplicity and efficiency. It depends only on the speed of the sprung mass which is affected by the type of road profile. The studied profile consists of a series of random roads selected according to the ISO 8608 standard. Only two measurements are required in the proposed coupling method: the sprung mass variation and the vehicle speed variation. The numerical results in time and frequency domain show that the modified ICA method ensures the passengers comfort and enhances the required performances.

Keywords Modified ICA · Semi-active control · Vehicle model · Passenger comfort

1 Introduction

Car manufacturers are considering ensuring the reliability of vehicles to avoid customer dissatisfaction, ensure their safety and provide the desired comfort. Since the automobile is subjected to different levels of vibration generated by different sources of excitation mainly the road roughness, it is equipped with a suspension system. This system has to ensure not only the comfort of the passenger but also allow for the control of the vehicle mainly in critical situations [1–3]. To this end, the customer's requirements for his driving comfort and the safety of modern cars are getting better and better. However, this represents a real challenge when designing the automobile. While improving these performances, designers integrate more components and subsystems into a single concept to provide more functionality and meet the customers' needs [4]. This increases the level of complexity of the suspension system [4]. For example, some researchers propose the use of pneumatic cylinders and controlled dampers to optimize comfort. However, all these concepts face a common limitation which is their inability to function properly until they are able to meet the imperfections of the road [4].

Recently, a semi-active suspension has been integrated into a vehicle with a look-ahead controller that is able to scan the road [5]. The road information will then be transferred to a cloud service for a change in the suspension damping. An adaptive hybrid control system is created to provide the value of the hybrid coefficient dynamically of semi-active suspension based on optimization of the performance of a classical hybrid control system. A new road estimator combined with a classification method was proposed [6, 7]. It aims to detect the road profile level referring to Adaptive Neuro fuzzy Inference System and wavelet transforms for adaptively change the control gains. A new fuzzy sliding mode controller with a disturbance estimator is introduced to improve semi active control performances in the presence of uncertainties related to the model errors and external disturbances [8].

Despite all these advantages, the aforementioned techniques are complicated and the tuning process is not straightforward. In addition, their implementation requires expensive equipment.

Technical Editor: Wallace Moreira Bessa.

✉ Dorra Ben Hassen
dorra.benhassen@yahoo.fr

[1] Mechanics, Modeling and Production Laboratory - National Engineering School of Sfax (ENIS), BP 1173–3038 Sfax, Tunisia

The road profile estimation is another aspect that has become crucial to allow better vehicle performances. In the literature, the road profile is the severe factor that influences the suspension dynamic response. For this reason, all the proposed strategies rely on identifying these exogenous sources to be used as additive information for changing the damping gains. The collection of information on the road profile is carried out using different techniques: Some, like the profile analyzer and the profilograph, use direct measurements [9, 10] while others are based on numerical estimation based on the knowledge of the vehicle dynamics. Recently, an online algebraic road profile estimator with straightforward calibration was proposed [11]. It just requires a specific choice of a sliding window to obtain better estimation results. Similarly, [12] suggested an online estimation method which uses the transmission characteristics of the vehicle and the estimation of the PSD of the road profile. The "Augmented Kalman filter" was applied to identify the road variability and proved the efficiency of this method to estimate the road profile. Nonetheless, it is sensitive to high vehicle speed variations [13]. As introduced by [14] another technique based on a statistical analysis of the dynamic response of the vehicle allows us to estimate road surface type. Then, the collected information will be integrated to an adaptive damping control technique for a vehicle suspension that facilitates the selection of the suspension damping setting.

Despite the many control and road profile identification methods investigated in the above-discussed research studies, there is still a scarcity of studies that integrate the road profile estimation in a control law. To achieve better vehicle performances, this paper aimed to integrate the road profile estimation into a semi-active suspension control. The Independent Component Analysis (ICA) was proposed as an estimation technique of the road profile [15, 16]. The advantage of the ICA is that it allows an easy identification of the excitation knowing the responses that can be measured by different sensors [17, 18]. The main idea of this paper was to integrate a switch control law in the ICA. Using the obtained modified algorithm, the influence of the estimated road on the choice of the suitable actuators will be taken into account since it is integrated into the controller. This controller acts accurately and at the right time to eliminate the vibrations due to the severity of the road profile. As a result, the ride comfort criterion is enhanced and the road holding is ameliorated. Furthermore, this coupling method is based on the use of the ICA for short periods of time (few seconds) to identify the real road among the different types of random roads defined by ISO 8608 [15] then switch automatically by choosing the adequate controller (specific gain for each type of road profile) in order to get the required performances.

The remaining of this paper is organized as follows: Sect. 2 described the system modeling. Sections 3 and 4 detailed the new coupling method, then, introduced the studied cases with the different types of road profile. In Sect. 5, we compared the passive and semi-active suspension systems to show the amelioration in the suggested system performance, on the one hand, and we carried out a robustness study of the coupling method using the sprung mass and the vehicle speed variation on the other hand. Section 6 was devoted to drawing the main conclusions.

2 System modeling

In this section, the quarter car model was studied. This model has two degrees of freedom as depicted in Fig. 1:

- X_i: the displacement of the sprung mass m
- y_j: the displacement of the tire m_1

This model is equipped by a skyhook control. Most of the studies indicate that this type of control is optimal in terms of its ability in isolating the suspended mass from basic excitations [4]. This control was achieved by using a simple speed feedback law, i.e., the speed of the suspended mass in the case of the quarter vehicle model. Hence, the force applied by the actuator is given by the following Eq. 1 [19]:

$$F_{\text{ai}} = -C_{\text{skyhook}}\dot{X}_i \tag{1}$$

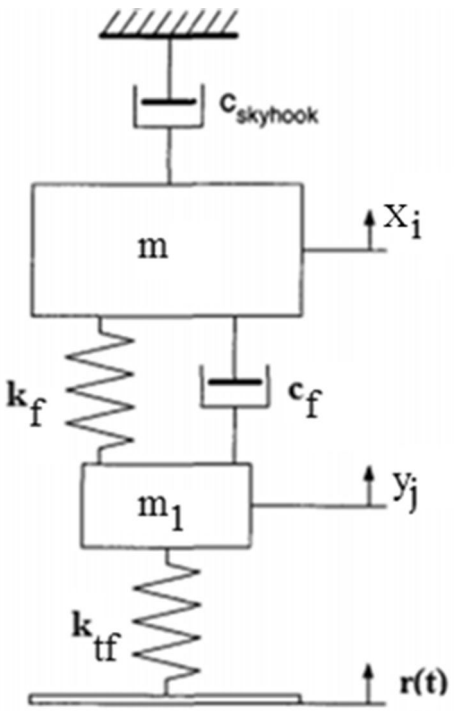

Fig. 1 Quarter vehicle model with skyhook damping

The equation of motion of the quarter car model is written as follows (Eq. 2):

$$\begin{cases} m\ddot{X}_i + k_f\left(X_i - y_j\right) + c_f\left(\dot{X}_i - \dot{y}_j\right) = F_{\text{ai}}(t) \\ m_1\ddot{y}_j + k_f\left(y_j - X_i\right) + c_f\left(\dot{y}_j - \dot{X}_i\right) + k_{\text{tf}}\left(y_j - r(t)\right) = -F_{\text{ai}}(t) \end{cases} \tag{2}$$

The choice of the quarter car model (Fig. 1) is based on the results of a previous article [15], which show that this model is the simplest and contains the basic characteristics of the full model but it can describe well a full model in terms of road profile estimation [15]. In order to slow down the motion of the vehicle, an opposite force to the direction of motion is produced. Since this is not possible in reality, we can make a controller to generate the Skyhook damping force. So, semi-active dampers which can vary depending on the type of excitation are used. The values of the gains chosen will depend on the type of the road profile. The values of the parameters used are presented in Table 1:

Remark The selection of suspension parameters is an important step. There are many assumptions that should be respected: Some references start by fixing natural frequencies of the sprung and unsprung masses [21] and then the value of damping ratio, can be determined. As we know when this constant is high, better driving dynamics are obtained. The lower this constant, the better is the comfort. In this first study the superiority is given for comfort.

However, it can be noted that, depending on road conditions, the damping ratio should be around 0.2 (for optimum ride) and 0.8 (for optimum handling) [22].

The road profile excitation is considered as random disturbances. The ISO 8608 standard assumes that the roads are classified in five main classes (from A to E) according to their roughness (Table 2) using this equation [16–23]:

$$\dot{y}_r(t) + w_0\, y_r(t) = \sqrt{Sg(\Omega_0).\, v.\, w(t)} \tag{3}$$

where y_r (t) is the road profile, v is the car velocity, w(t) is the noise signal and $w_0 = 0.2\pi$.v, S_g (Ω_0) is the road roughness.

Table 1 Parameters of the quarter vehicle model [20]

Parameters	Values	Unit
Sprung mass m	317.5	Kg
Unsprung mass m_1	45.4	Kg
Suspension stiffness k_f	20.000	N/m
Tire stiffness k_{tf}	192.000	N/m
Suspension damping c_f	535	Ns/m

Table 2 ISO road roughness classification

Road class	Roughness degree Sg(Ω_0) (10^{-6} m^2/cycle/m)	
	Range	Geometric mean
A (very good)	< 8	4
B (good)	8–32	16
C (Average)	32–128	64
D (poor)	128–512	256
E (very poor)	512–2048	1024

3 Classical ICA method

The ICA aims to reconstruct the source signal knowing only the vector of the observed signals written as in [24, 25]:

$$\{X\} = [A]\{S\} \tag{4}$$

with:

{X}: The vector of observed signals defined by the sprung mass acceleration in this study.

[A]: The mixing matrix.

{S}: The vector of source signals defined by the kinematic excitation.

The reconstruction process should be achieved under some assumptions given in [26] as follows:

- The vector {S} must have statistically independent components.
- The estimated sources and the observed signals must have the same number.
- The components of the vector S must have a non-Gaussian distribution.

Based on these assumptions, ICA computes the separating matrix $\left[W_s\right]$ which is equal to $[A]^{-1}$ after the centering and whitening the observed signals. Then, ICA estimates {S} using the deflection method [15, 16]. Estimated signals are written as:

$$\{S\} = \left[W_s\right]\{X\} \tag{5}$$

The computation of $\left[W_s\right]$ is based on the independence criterion defined by the maximization of the kurtosis (to guarantee the non-Gaussianity of the sources) as:

$$K = \frac{E\left\{|S|^4\right\} - 2E^2\left\{\left|S^2\right|\right\} - \left|E\left\{S^2\right\}\right|^2}{E^2\left\{\left|S^2\right|\right\}} \tag{6}$$

where E is the orthogonal matrix of eigenvectors of $E\left\{\mathrm{X}\,\mathrm{X}^T\right\}$.

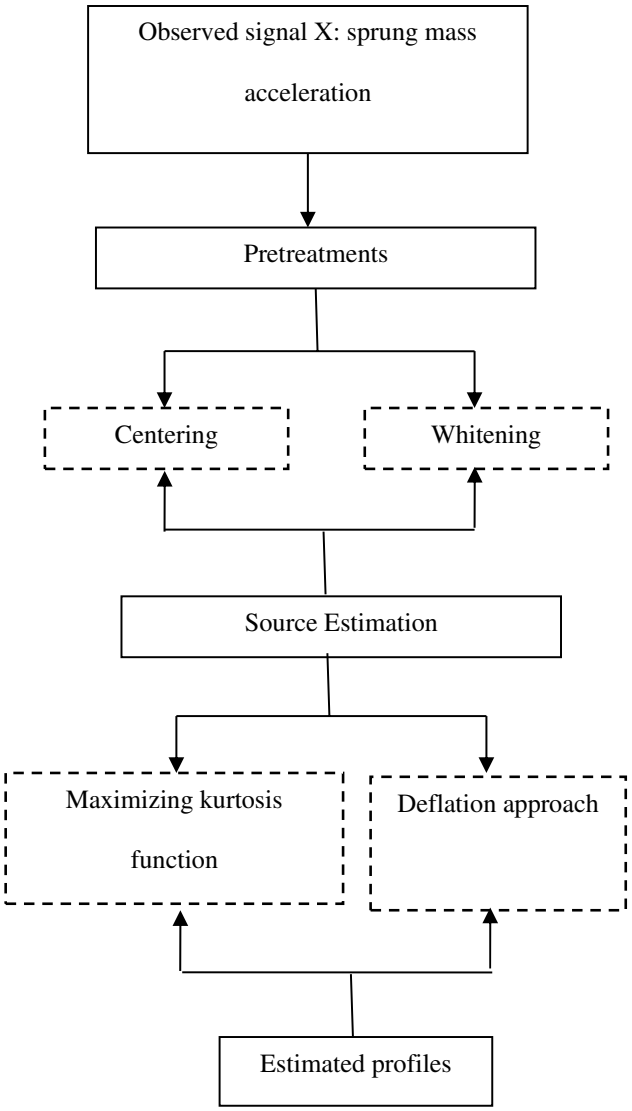

Fig. 2 Steps of road profile identification

The following diagram summers the steps of ICA to identify the road profile (Fig. 2)

4 A new modified ICA-algorithm

This method consists of an ICA-Control Coupling. In fact, in a real context, the vehicle is subjected to road disturbances caused by a succession of profiles (From A to E) as previously mentioned. Real-time road disturbance identification remains crucial for the application of the adequate controller for each disturbance. Indeed, the control takes into account the road variability and thus acts on the responses of the vehicle while ensuring the comfort of the passenger. It is therefore interesting to couple the

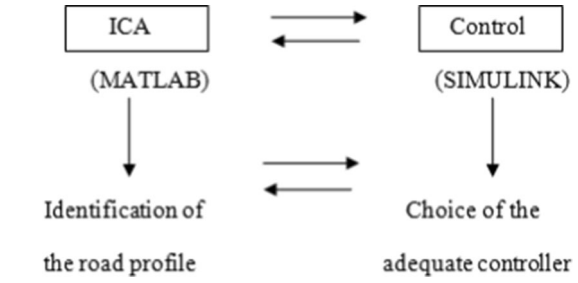

Fig. 3 ICA-Control Coupling

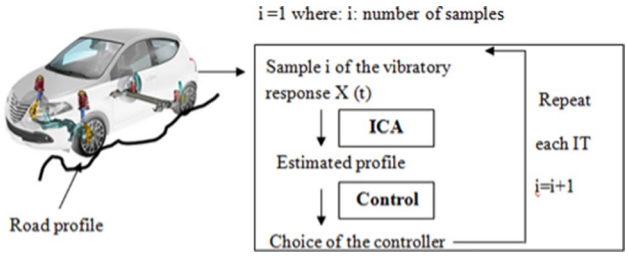

Fig. 4 Principle of the Coupling method

ICA with the control. This method makes it possible to identify the road profile variability by the ICA, on the one hand, and to choose the appropriate controller according to this estimated profile, on the other, to improve the performance of the vehicle. Figure 3 shows the coupling principle between the ICA and the control.

The vibratory response of the vehicle is influenced by the variability of the road profile. It is therefore necessary to examine this variation by taking samples of duration Δt and estimating periodically the road profile using the ICA. This estimation allows choosing the appropriate controller for each profile. This action will be repeated at each defined interval of time (IT). Experimentally, these samples are obtained by direct measurement from accelerometers; numerically, however, the vibratory responses of the studied model are calculated using Newmark method as described in a previous work [15]. Ultimately, it will be sampled. The principle of the method is presented in Fig. 4.

5 Numerical results

The results of the modified ICA algorithm are detailed in this section. In the first case, different types of random road profiles were generated to verify the effectiveness of the ICA method to estimate the true profile. Then, the robustness of the method was studied by varying the mass of the sprung (1st case) and the speed of the vehicle (2nd case). The evaluated performance criterion is the passenger comfort presented by the acceleration of the suspended mass.

The achieved results were compared to the ISO 2631–1 standard for assessing comfort. To ensure that the simplified model keeps up with the real car performance, the following assumptions and constraints were considered:

- The vehicle body and chassis are viewed as one rigid block and the desired performance criterion is the passenger comfort that is presented by the sprung mass acceleration. To evaluate the comfort obtained by the semi-active suspension the ISO2631-1 standard was used [27]. It is summarized in Table 3:
- It is assumed that the tires, springs and dampers are always perpendicular to the ground. In order to ensure driving safety and road holding stability, the dynamic load of the tire according to UESAMA criterion [28] should in no case exceed 80% of its static load.
- The four tires are always in contact with the ground.
- Considering the actuator saturation, the active control forces have upper limitation of 2000 N.

5.1 A sequence of road profiles with a constant vehicle speed

The kinematic excitation r(t) due to the road profile was constructed for a long road as follows: In the beginning, road A from 0 to 10 s; then, road B from 10 to 18 s; then, road C from 18 to 30 s; after that, road D from 30 to 40 s; finally, road E from 40 to 50 s. The vehicle speed is 15 m/s.

5.1.1 Estimated road profiles

Our estimation was performed on a sprung mass acceleration of duration of 50 s which was split into five intervals IT of 10 s each. The ICA was applied for samples of duration $\Delta t = 1$ s only, which means that we got 5 samples of duration 1 s as presented in Fig. 5.

Once the estimation was achieved, the identified profile was compared to the five profile types defined by ISO 8608

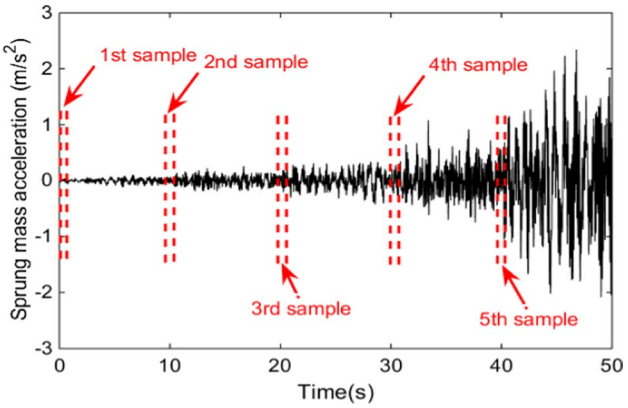

Fig. 5 Sprung mass acceleration with constant vehicle speed

by measuring the RMS of the Error (RMSE) between the estimated profile and the real one defined as:

$$\mathrm{RMSE} = \sqrt{\frac{\sum_{i=1}^{T} (S_r - S_e)^2}{T}} \tag{7}$$

where: S_r is the sample of real road profile.

S_e: Estimated road profiles.

T: Number of elements in the real and estimated vectors.

The smallest error corresponds to the profile identified by the ICA. The obtained results are summarized in Table 4.

The smallest error corresponds to the identified profile. From Fig. 6, it can be noticed that the ICA is able to reconstruct the true profile even from small samples of the observed signals X(t).

5.1.2 Selection of suitable controller gains

From each type of the identified profile, the corresponding controller is activated to improve the performance of the suspension system. The chosen gain values for each road profile are presented in Table 5 [20]. These values were chosen following several numerical trial and error tests. The obtained

Table 3 ISO2631-1 Standard [27]

RMS of acceleration (m/s^2)	Level of comfort
Less than 0.315	Comfortable
0.315 à 0.63	A little comfortable
0.5 à 1	Fairly uncomfortable
0.8 à 1.6	Uncomfortable
1.25 à 2.5	Very uncomfortable
Greater than 2.5	Extremely uncomfortable

Table 4 Identification of the road profile

RMSE	Road A	Road B	Road C	Road D	Road E
Samples					
1st sample	0.012	0.90	0.98	0.87	0.94
2nd sample	0.85	0.34	0.94	0.91	0.77
3rd sample	0.99	0.99	0.55	0.97	0.91
4th sample	0.84	0.93	0.94	0.23	0.98
5th sample	0.94	0.83	0.85	0.98	0.83

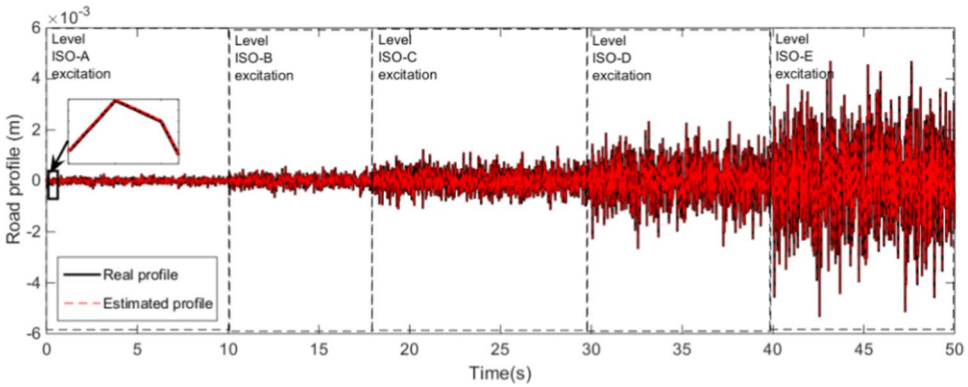

Fig. 6 Mixed random road profiles with constant speed: real and estimated profiles

Table 5 Values of chosen gains

Road profile level	A	B	C	D	E
Value of chosen gains (Ns/m)	680	750	2530	3820	4000

Table 6 Improvement of the suspension performance

Controller	RMS of the sprung mass acceleration (m/s^2)				
	Road A	Road B	Road C	Road D	Road E
Passive	0.038	0.09	0.174	0.36	0.72
Controller A	0.013	0.38	0.9	0.22	0.59
Controller B	0.014	0.047	0.069	0.21	0.43
Controller C	0.015	0.062	0.06	0.2	0.38
Controller D	0.015	0.065	0.075	0.15	0.38
Controller E	0.015	0.068	0.078	0.18	0.34

results show that each chosen gain is adequate only for one road profile type as shown in Table 6.

5.1.3 Required performances

As a required performance, the ride comfort presented by the sprung mass acceleration was chosen. It can be remarked that for a random road sequence, when the road levels vary, the skyhook controller performs well for each selected profile (Table 6). Thus the chosen gains are adequate for each type of well-defined road (Fig. 7).

Figure 7 shows the comparison between the passive and the semi-active systems in the time domain. From these results and the RMS values of Table 6, it can be noted that the ride comfort was improved by 63% for the profile type A, 47% for type B, 65% for type C, 58% for type D and 52% for type E. So, it can be said that while switching the controller from one road level to another its performance remains good. A suitable damping force is produced for attenuating unpredictable perturbations. Also, both of the road profile identification time and the controller choice take only 0.69 s. Therefore, it can be deduced that this coupling method is very advantageous in terms of simplicity and computation time.

On the other hand, the introduction of the modified ICA resulted in a good compromise between the vehicle ride comfort and the handling quality. As shown in Table 7 the tire holding has been ameliorated by 13% compared to the 2% achieved by the classical case. Nevertheless, the modified ICA control deteriorated the suspension working space by 20% [20].

To show the effectiveness of the proposed modified ICA, we activated the algorithm after 10 s in the case of the road profile type C and noted its influence on the ride comfort as shown in Fig. 8.

Obviously, the proposed controller with an online switching process needs more energy to offer suitable performances. However, the classical actuator produces a lower actuator force than the semi active with the modified ICA which can be justified by its inability to deal with the road profile change.

5.1.4 Frequency domain analysis

To further investigate the performance of the semi-active controller, the frequency domain response plots are displayed in Fig. 9. The bode diagrams of the typical transfer functions for sprung mass acceleration, the suspension deflection and the tire deflection with respect to different road perturbations are plotted. It can be seen that the gain of the vehicle sprung mass acceleration of the system with the proposed controller declined in the low frequency region and

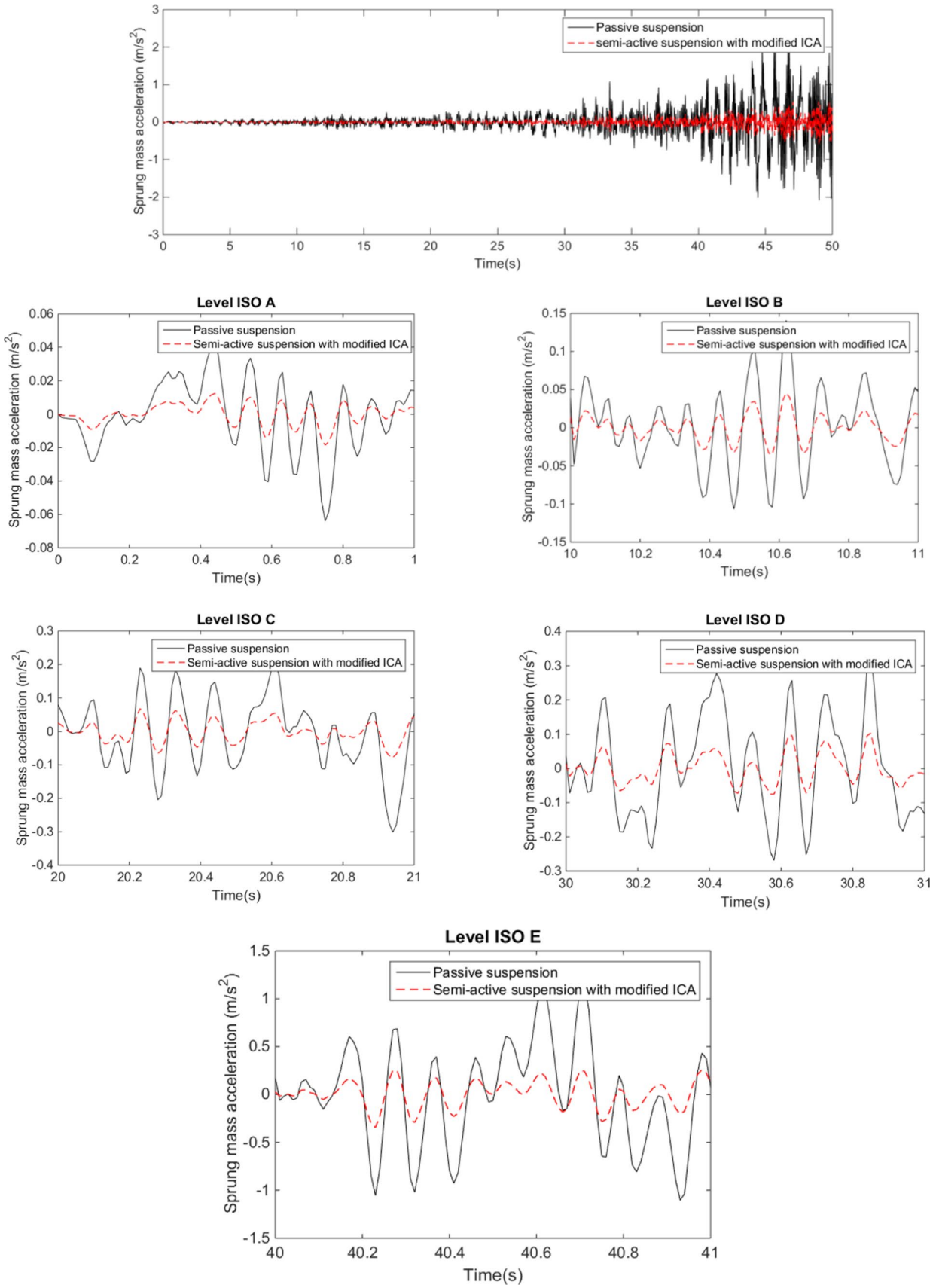

Fig. 7 Ride comfort improvement in passive and semi-active suspension system

Table 7 The suspension working space and the dynamic tire deflection performances

Road excitation	Suspension type	Suspension deflection (m)	Tire deflection (m)
Real profile	Passive	0.0204	0.0131
	Semi-active	0.0215 (↓ 5.4%)	0.0128 (↑ 2%)
Estimated profile	Passive	0.02	0.0138
	Semi-active (Modified ICA)	0.0251 (↓ 20%)	0.012 (↑ 13%)

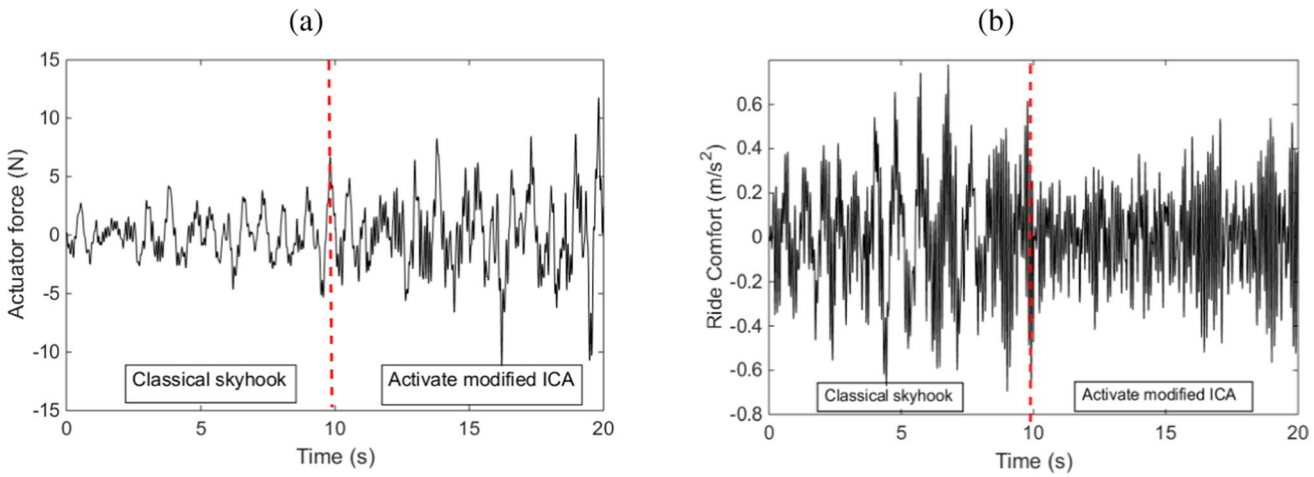

Fig. 8 **a** Actuator force in the case of classical and Modified skyhook **b** Sprung mass acceleration in the case of classical skyhook

then increased with the frequency increase. In the frequency range of interest 0–20 Hz, the first resonance peak was further attenuated with the modified ICA. From the above analysis, this improvement is related to the right selection of required damping added within the proposed algorithm. This analysis validates the correctness of the simulation results in the time domain that the power demand, which has a significant enhancement of the suspension performance in the observed features of the proposed controller depending on the type of road excitation.

5.2 Robustness analysis

Lastly, in this section, the sprung mass uncertainty and speed variation were considered to further discuss the robustness of proposed algorithm.

5.2.1 First case: road profile A-E-B-C-D with sprung mass variation

- Identification of the road profile

  In this case, a random profile consisting of the following road profiles, Road A—road E—road B—road C and finally road D, was used. A constant speed equal to 15 m/s was chosen. At a first case, any sprung mass

Table 8 Road profile identification with sprung mass variation

RMSE	Road A			Road B			Road C			Road D			Road E		
Sprung mass variation	0	20	40	0	20	40	0	20	40	0	20	40	0	20	40
Samples															
1st	0.012	0.022	0.05	0.9	0.93	0.95	0.98	0.99	1	0.87	0.88	0.92	0.94	0.94	0.98
2nd	0.95	0.97	1	0.85	0.87	0.92	0.74	0.79	0.83	0.98	0.99	1	0.002	0.05	0.07
3rd	0.85	0.87	0.9	0.34	0.42	0.48	0.94	0.96	0.98	0.91	0.93	0.96	0.77	0.78	0.81
4th	0.99	1	1	0.99	1	1	0.55	0.58	0.61	0.97	0.98	1	0.91	0.94	0.96
5th	0.84	0.89	0.92	0.93	0.94	0.97	0.94	0.95	0.97	0.23	0.26	0.32	0.98	0.99	1

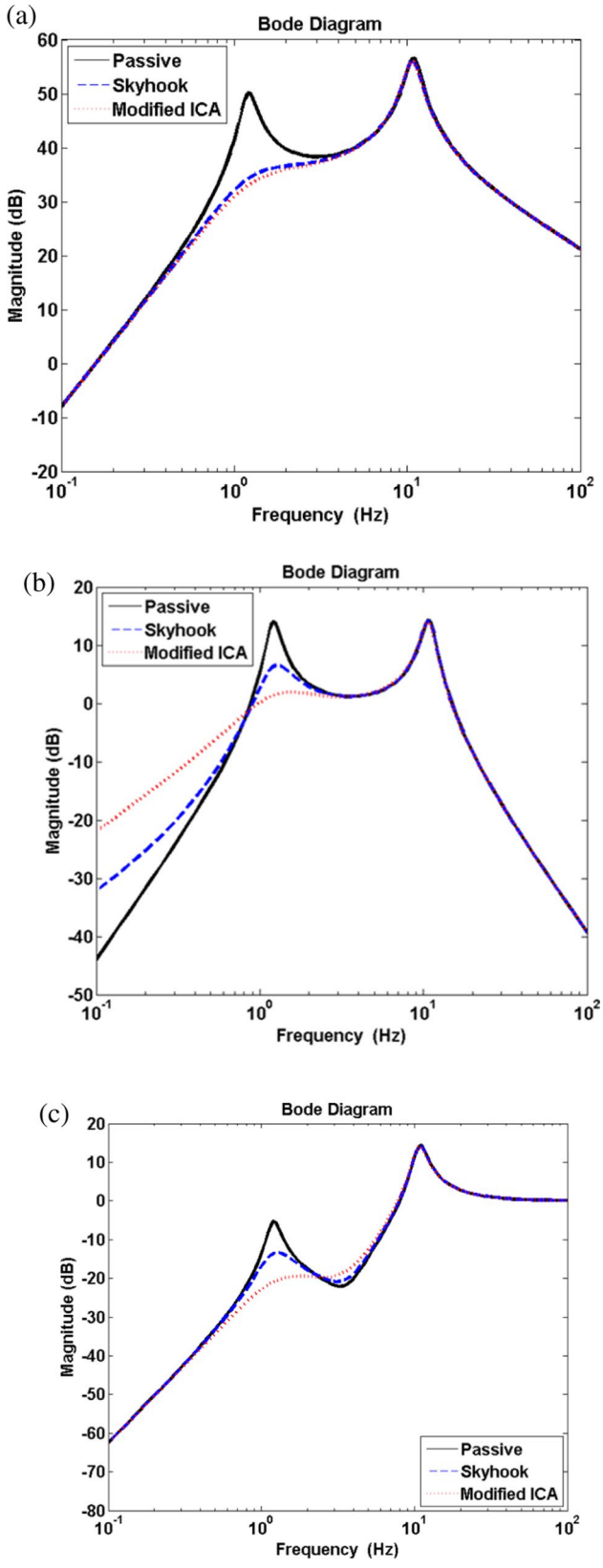

Fig. 9 Bode plots **a** Sprung mass acceleration **b** Suspension deflection and **c** tire deflection

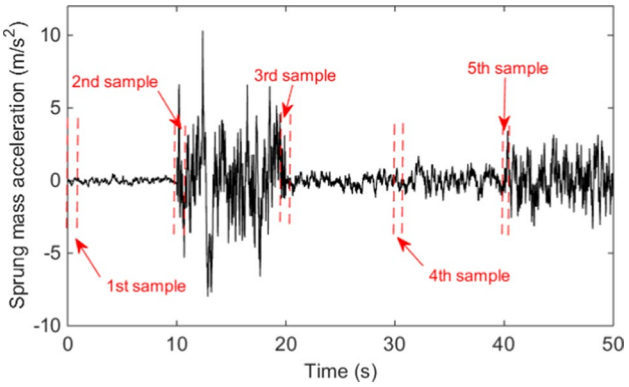

Fig. 10 Sprung mass acceleration without sprung mass variation

variation is applied, after that; variations of 20% and 40% were added to the actual mass of the vehicle to study their influence on the profile identification and the controller performance. Before applying the ICA to estimate this profile, the vector of the observed signals without sprung mass variation was calculated. It consists of the acceleration samples (Fig. 10).

The ICA profile identification errors results are shown in Table 8. The Root Mean Square Error (RMSE) defined previously by Eq. 7 is evaluated.

- Application of the controller

The corresponding controller for each profile type was activated after each estimation process. The achieved results are shown in Fig. 11 for the case of 20% variation and in Table 9 for the case of 40% variation.

It can be claimed that the obtained results are satisfactory since the required performance which is the ride comfort has been reached and that the modified ICA performs well in spite of the sprung mass variation.

5.2.2 2nd case: road profile C-B-E-D-A with variable speed

- Identification of the road profile

In this sub-section, the road profile was constructed by a series of random profiles Fig. 12 where we varied

Table 9 The ride comfort improvement using a 40% variation of the sprung mass

Controller	RMS of the sprung mass acceleration (m/s^2)				
	Road A	Road B	Road C	Road D	Road E
Passive	0.024	0.09	0.06	0.20	0.48
Controller A	0.011	0.039	0.051	0.098	0.32
Controller B	0.012	0.038	0.054	0.092	0.34
Controller C	0.012	0.039	0.05	0.094	0.32
Controller D	0.013	0.043	0.056	0.09	0.4
Controller E	0.014	0.045	0.058	0.11	0.3

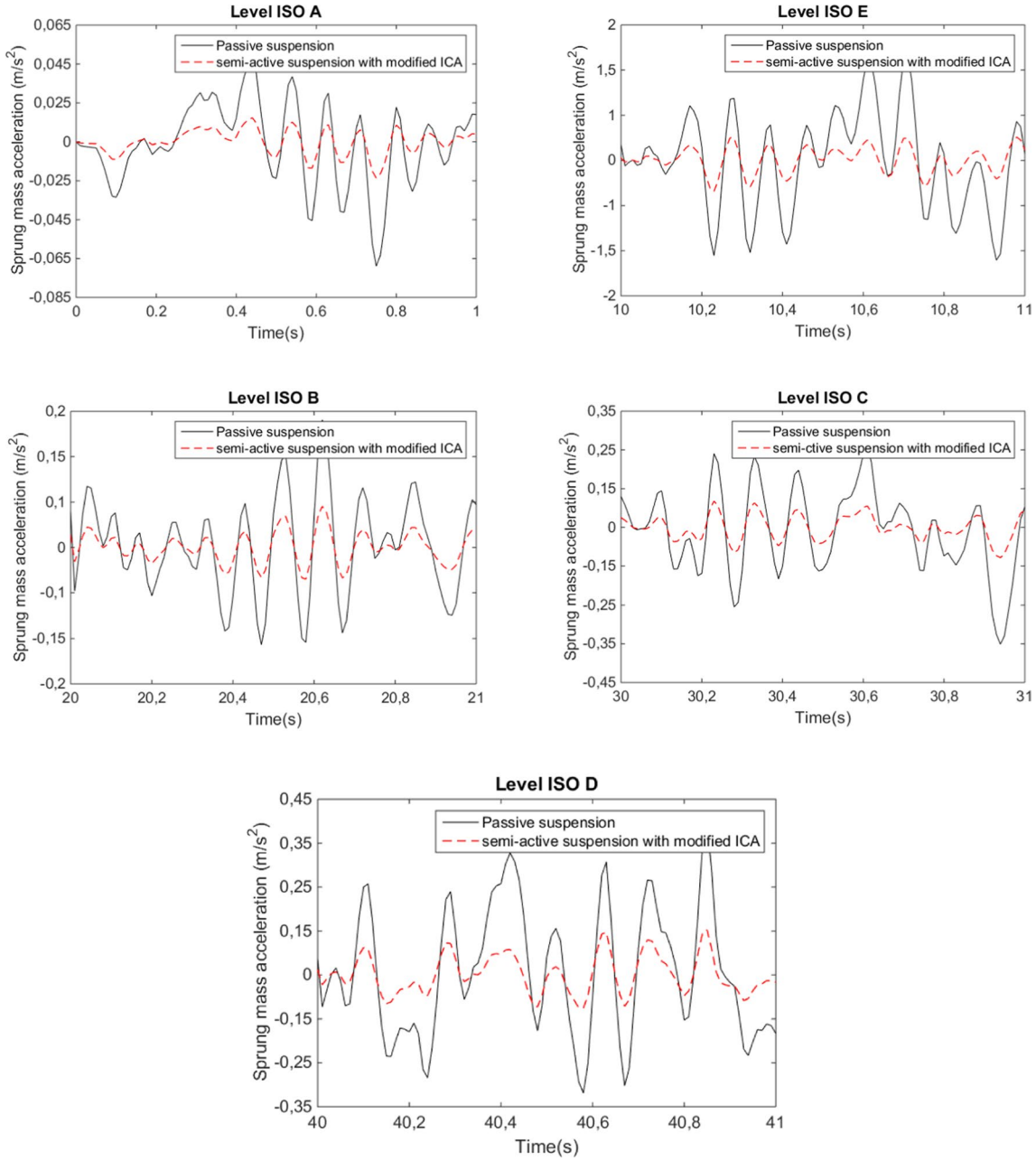

Fig. 11 Comparison between passive and semi-active suspension

Table 10 Road profile identification under vehicle speed variation

RMS of the error	Road C $V=15$ m/s	Road B $V=20$ m/s	Road E $V=10$ m/s	Road D $V=12$ m/s	Road A $V=25$ m/s
Samples					
1st sample	0.174	0.99	0.98	0.9	0.98
2nd sample	0.99	0.38	0.95	0.99	0.92
3rd sample	0.98	0.89	0.49	0.97	0.92
4th sample	0.89	0.99	0.97	0.85	0.99
5th sample	0.99	0.91	0.98	0.99	0.88

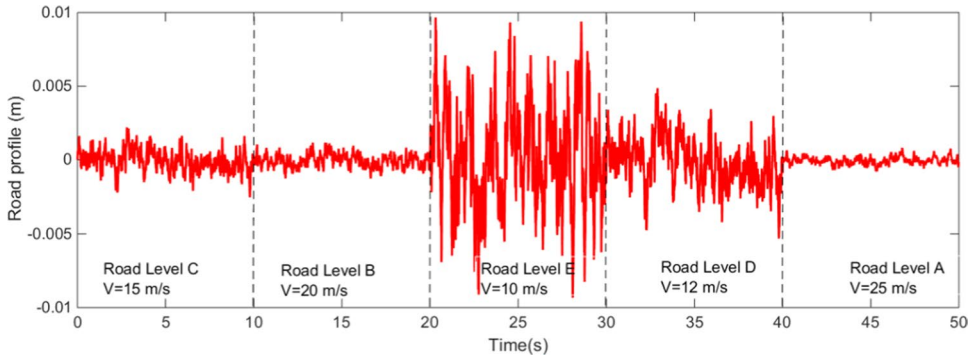

Fig. 12 Road profile with variable speed

Table 11 Improvement of the ride comfort under vehicle speed variation

Controller	RMS of the sprung mass acceleration (m/s^2)				
	Road C $V=15$ m/s	Road B $V=20$ m/s	Road E $V=10$ m/s	Road D $V=12$ m/s	Road A $V=25$ m/s
Passive	0.174	0.12	0.7	0.32	0.045
Controller A	0.16	0.07	0.39	0.131	0.025
Controller B	0.12	0.054	0.41	0.096	0.026
Controller C	0.058	0.057	0.22	0.09	0.026
Controller D	0.11	0.06	0.21	0.08	0.027
Controller E	0.11	0.064	0.2	0.09	0.028

the speed and kept the duration fixed at 10 s as follows: Road Level C 15 m/s; Road Level B 20 m/s; Road Level E 10 m/sec.; Road Level D 12 m/sec.; and Road Level A 25 m/sec. Table10 shows the results of the road profile identification.

According to the results displayed in Table 10, it can be noticed that the ICA was able to estimate the road profile even under the condition of speed variation.

- Application of the controller

Once the ICA has estimated the profile, the suitable controller of each road is applied in order to improve the performance. The obtained results are shown in Table 11:

The comparison between the semi-active and passive suspension systems performances allowed us to conclude that the first always yields better results taking into account the speed variation and the road imperfection. In addition, the required simulation time to identify the profile and activate the controller is just 0.73 s. Thus, this coupling method remains very interesting and really promising in enhancing the suspension performance.

6 Conclusion

In this paper, a new modified ICA algorithm was proposed in order to identify the road profile in real time and activate the suitable controller to improve the suspension performance.

The profile identification results are satisfactory. The ICA is able to reproduce the real profile even with a sample of 1 s of the sprung mass acceleration. Neither the speed nor the sprung mass variation affected the estimation process.

Using the skyhook control enabled us to enhance the vehicle performance. Thanks to this coupling method it was possible to use an online simple concept which is fast enough to detect the road profile variation and act on the adequate controller. Since, the efficiency of the algorithm is related to the driving speed (v) and the traveled distance (d), the response time of our algorithm should be lower than the ratio v/d which presents a limitation, especially when driving on a short way with high vehicle speed.

It can be noted that in this first study, the chosen passive damping coefficient is based on ensuring the passenger comfort. Such value can influence the choice of damping coefficient in the case of semi active suspension. If the parameters of passive damping would be bigger, one can obtain

different numeric results. So as perspective we propose to use an optimization algorithm to get the optimal value of passive damping.

Acknowledgements The authors would like to thank Dr. Vicente Zarzoso and Dr.Pierre Comon for conceiving the ICA algorithm [29].

References

1. AgharkakliA SGS, Barouz A (2012) Simulation and analysis of passive and active suspension system using quarter car model for different road profile. Int J Eng Trends Technol 3:636–644
2. Li P, Lam J, Cheung KC (2014) Multi-objective control for active vehicle suspension with wheelbase preview. J Sound Vib 333:5269–5282
3. Purushotham A (2013) Comparative simulation studies on MacPherson suspension system. Int J Mod Eng Res (IJMER) 3:1377–1381
4. TrabelsiH (2014) Contribution à la prise en compte d'exigences dynamiques en conception préliminaire de systèmes complexes. Dissertation. Châtenay-Malabry, Ecole centrale de Paris
5. Mihály A, Kisari Á, GáspárP NB (2019) Adaptive semi-active suspension design considering cloud-based road information. IFAC-Papers OnLine 52(5):249–254
6. Ranjan A, Prasanth S, Cherian F, Bhasker JP, Ravi K (2017) Adaptive hybrid control strategy for semi-active suspension system. In: IOP conference series: materials science and engineering Vol. 263, IOP Publishing, p. 062062
7. Qin Y, Dong M, Langari R, Gu L (2015) Guan J (2015) Adaptive hybrid control of vehicle semiactive suspension based on road profile estimation. Shock Vib 3:1–13
8. Song BK, An JH, Choi SB (2017) A new fuzzy sliding mode controller with a disturbance estimator for robust vibration control of a semi-active vehicle suspension system. Appl Sci 7(10):1053
9. Imine H, Delanne Y, M'sirdi NK (2006) Road profile input estimation in vehicle dynamics simulation. Veh Syst Dyn 44(4):285–303
10. Materials ASoT (2003) Standard test method for measuring pavement roughness using a profilograph. West Conshohocken (PA): ASTM Int
11. Haddar M et al (2019) Road profile identification with an algebraic estimator. Proc Inst Mech Eng C J Mech Eng Sci 233(4):1139–1155
12. Liu W, Wang R, Ding R, Meng X, Yan L (2020) On-line estimation of road profile in semi-active suspension based on unsprung mass acceleration. Mech Syst Signal Process 135:106370
13. Fauriat W et al (2016) Estimation of road profile variability from measured vehicle responses. Veh Syst Dyn 54(5):585–605
14. K Dbrowski, G laski (2016) Method and algorithm of automatic estimation of road surface type for variable damping control. In IOP conference series: materials science and engineering (Vol. 148, No. 1, p. 012028). IOP Publishing
15. Ben Hassen D et al (2017) Road profile estimation using the dynamic responses of the full vehicle model. Appl Acoust 147:87–89
16 Chaabane MM et al (2019) Road profile identification using the estimation techniques: comparison between independent component analysis and Kalman filter. J Theo Appl Mech. https://doi.org/10.15632/jtam-pl/104592
17. Akrout A et al (2012) Estimation of dynamic system's excitation forces by the independent component analysis. Int J Appl Mech 4(03):1250032
18. Taktak M et al (2012) One stage spur gear transmission crankcase diagnosis using the independent components method. Int J Veh Noise Vib 8:387–400
19. Rajamani R (2011) Vehicle dynamics and control. Springer Science & Business Media
20. Wang R et al (2021) Switching control of semi-active suspension based on road profile estimation. Veh Syst Dyn. https://doi.org/10.1080/00423114.2021.1889621
21. Jazar RN (2014) Quarter car model vehicle dynamics. Springer, New York, pp 985–1026
22. Ślaski G (2011) Damping parameters of suspension of passenger vehicle equipped with semi-active dampers with by-pass valve. Transp Probl 6:35–42
23. HasbullahF et al (2015) Ride comfort performance of a vehicle using active suspension system with active disturbance rejection control. Int J Veh Noise Vib 11(1):78–101
24. Jutten C, Herault J (1991) Blind separation of sources, part I: an adaptive algorithm based on neuromimetic architecture. Signal Process 24:1–10
25. Comon P (1994) Independent component analysis, a new concept? Signal Process 36:287–314
26. Hyvärinen A, Oja E (2000) Independent component analysis: algorithms and applications. Neural Netw 13:411–430
27. Bouazara M (1997) Étude et analyse de la suspension active et semi-active des véhicules routiers Dissertation. Thèse de doctorat Présentée à la faculté des études supérieurs de l'université Laval à Québec, pour l'obtention du grade de PhilosophiaeDoctor en génie mécanique.
28. Lozia Z, Zdanowicz P (2018, September) Simulation assessment of the impact of inertia of the vibration plate of a diagnostic suspension tester on results of the EUSAMA test of shock absorbers mounted in a vehicle. In IOP Conference Series: Materials Science and Engineering, Vol. 421, p 022018
29. Zarzoso V, Comon P (2010) Robust independent component analysis by iterative maximization of the kurtosis contrast with algebraic optimal step size. IEEE Trans Neural Netw 21:248–261